A Computationally Efficient Method to Design Probabilistically Robust Wide-Area PSSs for Damping Inter-Area Oscillations in Wind Integrated Power Systems

J. S. Zhou, D. P. Ke, C. Y. Chung, *Fellow, IEEE,* and Y. Z. Sun, *Senior Member, IEEE*

***Abstract*--This paper proposes an efficient method that tunes wide-area power system stabilizers (WPSSs) to have probabilistic robustness for damping inter-area electro-mechanical oscillations in power systems with incorporated random wind power. Specifically, the efficiency of this method benefits from unique consideration and deduction of the analytic forms of cumulative distribution functions (cdfs) of two types of random variables and their derivatives with respect to tunable parameters of the conventionally structured WPSSs, based on approximations of wind power probability density functions by Gaussian mixtures. These cdfs then compose the objective function of an optimization that can rapidly solve for optimal parameters of WPSSs by a sequential quadratic programming algorithm. The optimized WPSSs are probabilistically robust because they enhance the probability of two commonly desired control effects. Simulation studies on a modified IEEE 10-machine and 39-bus system validate the superior efficiency of the proposed tuning method and the excellent performance of the derived WPSSs.**

***Index Terms*--Gaussian mixture, mathematical programming, probability, robust, wide-area power system stabilizer.**

I. Introduction

THE steady-state operating point of a power system that accommodates a large amount of wind power generally varies stochastically. Specifically, the small signal stability characteristics associated with electromechanical oscillations of the power system are possibly quite different over the many wind-induced operating points [1]-[3]. Damping controllers are designed to use local information of an operating point to acquire a certain robustness in the vicinity of this point; however, they might have very weak immunity against wind power variations because they are inherently blind to the entire region of the operating point. In other words, it is important to consider stochastic variations of wind power during the design of damping controllers to obtain robustness that is effective over a much larger region.

Studies of damping control designs that employ multiple operating points generated by variable wind power have already been conducted, e.g., [4]. It is noted that these studies fit the general idea of the conventional robust design which attempts to obtain a favorably-sized feasible region and all required control effects are satisfied by the resulting controllers if the operating point is inside this region. In other words, the conventional robustness clearly indicates the size of the above mentioned feasible region where the operating point only possibly appears due to its randomness nature. Although the calculation of this region can be carried out without knowing any information of probability, the conventional robust design may give rise to conservative design results. This is because damping controllers are preferably designed to meet all control requirements at each point of a region where the operating point has a large probability to show up during practical operation. Obviously, the resulting region is unnecessarily as large as the one derived by the conventional robust design and its size (or shape) is apparently determined by the random sources (e.g. wind power) affecting the operating point. Hence, the resulting damping controllers are regarded to be with probabilistic robustness. Such a design philosophy is noted in [5], where synthesized damping controllers for a nominal operating point are identified depending on the probability distributions of open-loop eigenvalues. Moreover, [6] uses probabilistic observability and controllability indexes to select damping controller inputs and outputs as another approach to consider the randomness of an operating point. The above design philosophy is exhibited in [7], where an optimization-based approach is proposed to tune damping controllers with the objective of maximizing the probability of desired control effects. Hence, the derived damping controllers are probabilistically robust against wind power variations. However, an obvious insufficiency of the method in [7] is low efficiency when searching for optimal parameters of the damping controllers because evaluation of the objective function by a Latin hypercube sampling (LHS) technique must be repeated a number of times by a customized particle swarm optimization (PSO). Specifically, [8] employs an analogous objective function that can be approximately calculated in an analytical manner based on the assumption that damping ratios of concerned modes obey normal distributions. Even so, the optimization of damping controller parameters in [8] is still solved by PSO with relatively low efficiency.

Accordingly, among the various research issues relevant to the design of damping controllers with probabilistic robustness, the computational efficiency of the design method is an important point for which there remains considerable room for improvement. To achieve this goal, analytical approaches, rather than time-consuming sampling techniques (e.g., LHS), seem indispensable for handling the randomness of wind power. Indeed, apart from the method in [8], several other analytical methods can more accurately derive the probability density function (pdf) and cumulative distribution function (cdf) of a

This work was supported by the Natural Science Foundation of China (Grant No.: 51777143). J. S. Zhou, D. P. Ke (corresponding author), and Y. Z. Sun are with the School of Electrical Engineering, Wuhan University, Wuhan 430072, China (zhoujingsen@whu.edu.cn, kedeping@whu.edu.cn).

C. Y. Chung is with the Department of Electrical and Computer Engineering, University of Saskatchewan, Saskatoon, Canada (c.y.chung@usask.ca).

mode's (eigenvalue's) damping (or damping ratio), such as the cumulants-based method in [9] and the mixture of joint Gaussian functions in [10]. Although these methods are able to efficiently accomplish the probabilistic computations, how to incorporate them into the above-mentioned stochastic decision problem (i.e., tuning damping controllers to obtain probabilistic robustness) has not been reported.

To suppress inter-area oscillations in wind integrated power systems, this paper proposes an optimization-based method to search optimal parameters of conventionally structured wide-area power system stabilizers (WPSSs). The desired probabilistic robustness is derived because the optimized damping controllers can enhance the probability that concerned inter-area modes satisfy the required damping ratios and that frequency changes caused by the WPSSs are less than specified values. In contrast to existing studies, the proposed damping control design is unique because it considers the cdfs of two specific kinds of random variables, together with their derivatives with respect to tunable parameters of the WPSS, and performs the analytical deduction with quite high accuracy; the optimization with the objective function formed based on these cdfs is therefore very efficiently solved by a gradient-descent algorithm (i.e., sequential quadratic programming, SQP). It should be emphasized that the above analytic deductions of the cdfs and their derivatives are based on approximation of the wind power pdf by a linear combination of three Gaussian functions (Gaussian mixtures) [11].

The remainder of the paper is organized as follows. Section II introduces the Gaussian mixtures method to approximate the randomness of wind power. Based on this approximation, Section III deduces the analytic forms of the cdfs for two types of random variables and their derivatives. Section IV uses these cdfs to construct the optimization, which is solved by the SQP method. Simulations and analysis are presented in Section V. Section VI concludes the paper.

II. Approximating the PDF of Wind Power Generation by a Linear Combination of Three Gaussian Functions

Fast computation of the probability distribution of an eigenvalue (as well as derivatives of this distribution) with necessary accuracy is remarkably relevant to the ultimate objective of this paper, i.e., efficient and effective tuning of damping controller parameters to satisfactorily suppress inter-area power oscillations. Hence, because the randomness of eigenvalues is induced by integrated wind power, a dedicated approach rather than a general sampling technique (e.g., LHS) is required to skillfully deal with (or express) the probability distribution of wind power generation (WPG).

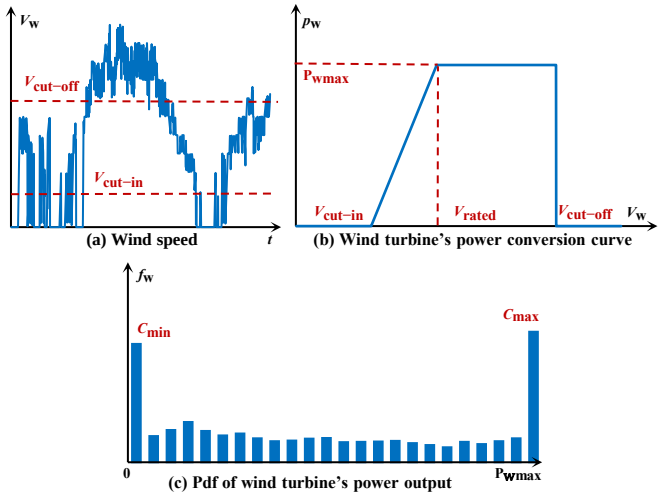

Fig.1. Basic procedure to derive the pdf of a wind turbine's power output

Fig. 1 illustrates the basic procedure for deriving the pdf ($f_w(\cdot)$) of a wind turbine's power output (p_w). A common feature of the pdf is observed: two impulses appear at discontinuous points 0 and p_{wmax} (the rated power of the wind turbine). Such a pdf cannot be directly included in the analytic probability calculation, but its approximation is generally employed, such as in the previously mentioned cumulants-based method. However, this feature of the pdf is an obstacle even for a high order cumulants-based method to obtain a feasibly accurate approximation [12], [13]. Therefore, a dedicated approximation approach that can specifically handle the impulses and discontinuities of the pdf is applied in this paper [11]. Because impulse function $\delta(x)$ and Gaussian function $g(x, \mu, \sigma)$ will be used for the approximation, their properties are outlined first, as follows:

$$\int_{x_0^-}^{x_0^+} c\delta(x-x_0)dx = c \tag{1}$$

$$\delta(x-x_0) = 0, x \neq x_0 \tag{2}$$

$$g(x,\mu,\sigma) = \frac{1}{\sigma\sqrt{2\pi}} e^{-\frac{1}{2}\left(\frac{x-\mu}{\sigma}\right)^2} \tag{3}$$

$$\int_{-\infty}^{\infty} g(x,\mu,\sigma) = 1 \tag{4}$$

where c and x_0 denote the strength and position, respectively, of the impulse; and μ and σ are the expectation and standard deviation, respectively, of the Gaussian function. As σ becomes smaller, the peak of the bell curve associated with the Gaussian function increases while the bottleneck narrows. In the extreme case (σ=0), the Gaussian function is equal to an impulse function with a strength of one. In other words, an impulse function can be regarded as a Gaussian function with a standard deviation equal to zero.

In this paper, all wind turbines in a wind farm are assumed to have the same parameters. Thus, the pdf shown in Fig. 1 is used to denote the pdf of the farm's WPG. According to [11], the two impulses are directly preserved in an approximation of the pdf, as follows:

$$\begin{aligned} f_w^{(j)}(p_w^{(j)}) = {} & c_{max}^{(j)}\delta(p_w^{(j)} - p_{w\,max}^{(j)}) \\ & + c_{min}^{(j)}\delta(p_w^{(j)}) + c_g^{(j)} g(p_w^{(j)}, \mu_g^{(j)}, \sigma_g^{(j)}) \end{aligned} \tag{5}$$

where the superscript '(j)' denotes the symbols or variables corresponding to the jth wind farm. In (5), $c_{max}^{(j)}$, $c_{min}^{(j)}$, and $p_{wmax}^{(j)}$ are known constants as shown in Fig. 1 while $c_g^{(j)}$, $\mu_g^{(j)}$, and $\sigma_g^{(j)}$ must be sequentially solved from the following equations, where the zero-, first-, and second-order moments are respectively coincident between the real pdf and its approximation:

$$c_{\max}^{(j)} + c_{\min}^{(j)} + c_{g}^{(j)} = 1 \tag{6}$$

$$c_{\max}^{(j)} p_{w\max}^{(j)} + c_{g}^{(j)} \mu_{g}^{(j)} = \mu_{w}^{(j)} \tag{7}$$

$$c_{\max}^{(j)} \left(p_{w\max}^{(j)}\right)^2 + c_{g}^{(j)} \left[\left(\mu_{g}^{(j)}\right)^2 + \left(\sigma_{g}^{(j)}\right)^2\right] = \left(\mu_{w}^{(j)}\right)^2 + \left(\sigma_{w}^{(j)}\right)^2 \tag{8}$$

where $\mu_{w}^{(j)}$ and $\sigma_{w}^{(j)}$ are the expectation and standard deviation of the jth wind farm's power output, respectively, and can be statistically derived based on historical wind speed data and the power conversion curve of the wind farm as shown in Fig. 1. Moreover, the probability distribution of the wind farm's power output can also be equivalently represented by the pdf of the power output deviation with respect to the expected power output (i.e., $\mu_{w}^{(j)}$), as follows:

$$\begin{aligned} f_{w}^{(j)}(\Delta p_{w}^{(j)}) &= c_{\max}^{(j)} \delta(\Delta p_{w}^{(j)} - p_{w\max}^{(j)} + \mu_{w}^{(j)}) \\ &+ c_{\min}^{(j)} \delta(\Delta p_{w}^{(j)} + \mu_{w}^{(j)}) + c_{g}^{(j)} g(\Delta p_{w}^{(j)}, \mu_{g}^{(j)} - \mu_{w}^{(j)}, \sigma_{g}^{(j)}) \end{aligned} \tag{9}$$

$$\Delta p_{w}^{(j)} = p_{w}^{(j)} - \mu_{w}^{(j)} \tag{10}$$

Furthermore, considering the equivalence between the Gaussian function with zero deviation and the impulse function, (9) can be rewritten in a more compact form, as follows:

$$f_{w}^{(j)}(\Delta p_{w}^{(j)}) = \sum_{t=1}^{3} c_{t}^{(j)} g\left(\Delta p_{w}^{(j)}, \mu_{t}^{(j)}, \sigma_{t}^{(j)}\right) \tag{11}$$

$$\begin{aligned} &c_1^{(j)} = c_{\max}^{(j)} && c_2^{(j)} = c_{\min}^{(j)} && c_3^{(j)} = c_g^{(j)} \\ &\mu_1^{(j)} = p_{w\max}^{(j)} - \mu_{w}^{(j)} && \mu_2^{(j)} = -\mu_{w}^{(j)} && \mu_3^{(j)} = \mu_{g}^{(j)} - \mu_{w}^{(j)} \\ &\sigma_1^{(j)} = 0 && \sigma_2^{(j)} = 0 && \sigma_3^{(j)} = \sigma_{g}^{(j)} \end{aligned} \tag{12}$$

In (11), the pdf is approximated by a linear combination of three Gaussian functions. In this paper, it is hypothesized that n_w wind farms have mutually independent power outputs. Analogously, each wind farm's pdf can be approximated in the form of (11). Specifically, the vectors $\boldsymbol{p}_w$, $\bar{\boldsymbol{p}}_w$, and $\Delta\boldsymbol{p}_w$, which are used for the convenient presentation of subsequent calculations, consist of $p_{w}^{(j)}$, $\mu_{w}^{(j)}$, and $\Delta p_{w}^{(j)}$ (j=1, 2, …, n_w), respectively. Moreover, it is assumed that all wind farms output expected power ($\boldsymbol{p}_w$=$\bar{\boldsymbol{p}}_w$) at the nominal operating point.

III. Two Types of Random Variables Used for Damping Control Design and Their CDFs

This section introduces two types of random variables as the foundation for constructing the optimization used for tuning damping controllers (Section IV). The significance here is that the cdfs of these variables are approximately yet analytically calculated based on the description of WPG's randomness from the above Gaussian mixtures. However, the decentralized damping control structure employed in this paper is first introduced to facilitate demonstration of those calculations. The PSSs are installed locally in synchronous generators, each with the conventional structure consisting of gain and phase lead-lag blocks and using the wide-area signal as the input. Fig. 2 illustrates the block diagram of the mth PSS, where y_m denotes the wide-area signal and v_m is the supplementary excitation signal of the synchronous generator. Specifically, the gain (K_m) and time constants (T_{1m}, T_{2m}, T_{3m}, T_{4m}) of the PSSs are the parameters to be tuned in this study.

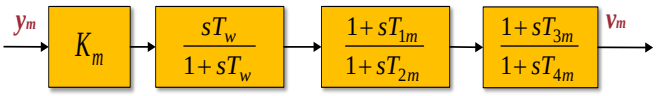

Fig. 2. Control structure of the mth PSS

These PSSs can be synthesized to a single state-space representation, as follows:

$$\dot{\boldsymbol{x}}_c = \boldsymbol{A}_c(\boldsymbol{q})\boldsymbol{x}_c + \boldsymbol{B}_c(\boldsymbol{q})\boldsymbol{y}_c \tag{13}$$

$$\boldsymbol{u} = \boldsymbol{C}_c(\boldsymbol{q})\boldsymbol{x}_c + \boldsymbol{D}_c(\boldsymbol{q})\boldsymbol{y}_c \tag{14}$$

where $\boldsymbol{x}_c$ is the state vector consisting of all of the PSSs' state variables, and $\boldsymbol{y}_c$ and $\boldsymbol{u}$ are the output and input vectors with components y_1, y_2, …, y_{nc} and v_1, v_2, …, v_{nc} (n_c is the number of PSSs), respectively. Detailed derivation of the matrices $\boldsymbol{A}_c$, $\boldsymbol{B}_c$, $\boldsymbol{C}_c$, and $\boldsymbol{D}_c$ can be found in [14], noting that they are exclusively calculated from the damping controllers' parameters so that they are parameterized by the tunable parameter vector $\boldsymbol{q}$, as follows:

$$\boldsymbol{q} = [K_1,...,K_{nc},T_{11},...,T_{1nc},T_{21},...,T_{2nc},T_{31},...,T_{3nc},T_{41},...,T_{4nc}] \tag{15}$$

Moreover, it is easily understood that $\boldsymbol{A}_c$, $\boldsymbol{B}_c$, $\boldsymbol{C}_c$, and $\boldsymbol{D}_c$ have no relationship with the power system operation.

The open-loop power system can be linearized at an operating point to obtain the state-space equations, as follows:

$$\dot{\boldsymbol{x}}_o = \boldsymbol{A}_o(\boldsymbol{p}_w)\boldsymbol{x}_o + \boldsymbol{B}_o(\boldsymbol{p}_w)\boldsymbol{u} \tag{16}$$

$$\boldsymbol{y}_o = \boldsymbol{C}_o(\boldsymbol{p}_w)\boldsymbol{x}_o \tag{17}$$

where $\boldsymbol{x}_o$ is the state vector of the open-loop power system. The matrices $\boldsymbol{A}_o$, $\boldsymbol{B}_o$, and $\boldsymbol{C}_o$ are computed depending on the operating point. Moreover, it is assumed that the open-loop power system operating point is subjected to smooth variations because of the WPG ($\boldsymbol{p}_w$). Therefore, $\boldsymbol{A}_o$, $\boldsymbol{B}_o$, and $\boldsymbol{C}_o$ are parameterized by $\boldsymbol{p}_w$ while they are independent of the damping controllers' parameters. Particularly, this study assumes that a same doubly-fed induction generator (DFIG) based wind turbine aggregately represents each wind farm. More information about the dynamical model of DFIG based wind turbine is presented in Appendix. Obviously, the above open-loop power system model has incorporated all the aggregated wind turbines' models.

Communication time delays induced by the use of wide-area signals are explicitly considered in the damping control design. In general, the time delay is stochastically variable and it is exclusively determined by the communication system. In this study, it is supposed that the dedicated optical-fiber channel is used for the communication so that the relevant time delay can quite possibly vary within a small range [15]. Under such circumstance, the time delay is simply regarded to be constantly its expected value. Then, in the Laplace domain the expected time delay has an exponential form which can be approximated by a second-order Pade formula, as follows [16]:

$$e^{-\tau s} \approx \frac{\tau^2 s^2 - 6\tau s + 12}{\tau^2 s^2 + 6\tau s + 12} \tag{18}$$

where τ is the time delay. Thus, when time delays existing in all feedback control loops are respectively approximated by (18), their dynamics can be alternatively described by the following state space equations:

$$\dot{\boldsymbol{x}}_{\mathrm{t}} = \boldsymbol{A}_{\mathrm{t}}\boldsymbol{x}_{\mathrm{t}} + \boldsymbol{B}_{\mathrm{t}}\boldsymbol{y}_{\mathrm{o}} \tag{19}$$

$$\boldsymbol{y}_{\mathrm{c}} = \boldsymbol{C}_{\mathrm{t}}\boldsymbol{x}_{\mathrm{t}} + \boldsymbol{D}_{\mathrm{t}}\boldsymbol{y}_{\mathrm{o}} \tag{20}$$

where $\boldsymbol{x}_{\mathrm{t}}$ is the state vector of the approximated time delays. The matrices $\boldsymbol{A}_{\mathrm{t}}$, $\boldsymbol{B}_{\mathrm{t}}$, $\boldsymbol{C}_{\mathrm{t}}$ and $\boldsymbol{D}_{\mathrm{t}}$ are computed by transferring (18) to the state space form.

Based on (13)-(14), (16)-(17) and (19)-(20), the state matrix $\boldsymbol{A}_{\mathrm{cp}}$ of the closed-loop power system is obtained by combining the models of the damping controllers, the open-loop power system and the time delays, as follows:

$$\boldsymbol{A}_{\mathrm{cp}} = \begin{bmatrix} \boldsymbol{A}_{\mathrm{o}} + \boldsymbol{B}_{\mathrm{o}}\boldsymbol{D}_{\mathrm{c}}\boldsymbol{D}_{\mathrm{t}}\boldsymbol{C}_{\mathrm{o}} & \boldsymbol{B}_{\mathrm{o}}\boldsymbol{D}_{\mathrm{c}}\boldsymbol{C}_{\mathrm{t}} & \boldsymbol{B}_{\mathrm{o}}\boldsymbol{C}_{\mathrm{c}} \\ \boldsymbol{B}_{\mathrm{t}}\boldsymbol{C}_{\mathrm{o}} & \boldsymbol{A}_{\mathrm{t}} & \boldsymbol{0} \\ \boldsymbol{B}_{\mathrm{c}}\boldsymbol{D}_{\mathrm{t}}\boldsymbol{C}_{\mathrm{o}} & \boldsymbol{B}_{\mathrm{c}}\boldsymbol{C}_{\mathrm{t}} & \boldsymbol{A}_{\mathrm{c}} \end{bmatrix} \tag{21}$$

For expression simplicity, the parameterization denotations '($\boldsymbol{q}$)' and '($\boldsymbol{p}_{\mathrm{w}}$)' are omitted in (21). Subsequently, the two types of random variables and computations of their cdfs are presented in the following subsections based upon the above information for the damping controllers.

A. Damping of Critical Inter-Area Mode and Calculation of its Probability Distribution

One type of random variable of concern is the real part (damping) of a weakly damped (critical) inter-area mode. Generally, the damping of the *i*th critical inter-area mode can be decomposed in the following form:

$$\alpha_i = \alpha_{i0}(\boldsymbol{q}) + \Delta\alpha_i(\boldsymbol{q},\ \Delta\boldsymbol{p}_{\mathrm{w}}) \tag{22}$$

where α_{i0} is the damping at the nominal operating point (i.e., all WPG are with respective expected values, $\boldsymbol{p}_{\mathrm{w}}$=$\bar{\boldsymbol{p}}_{\mathrm{w}}$) determined by the damping controllers' tunable parameters; and $\Delta\alpha_i$ denotes the deviation of the damping with respect to α_{i0} as the operating point ($\boldsymbol{p}_{\mathrm{w}}$) deviates from the nominal one ($\bar{\boldsymbol{p}}_{\mathrm{w}}$). Specifically, for a given $\boldsymbol{q}$, α_{i0} will be constant while $\Delta\alpha_i$ is the differentiable function of the wind power deviations ($\Delta\boldsymbol{p}_{\mathrm{w}}$). In fact, (22) can be regarded as the Taylor series expansion of α_i with respect to $\Delta\boldsymbol{p}_{\mathrm{w}}$; thus, if the terms with orders equal to or higher than two are neglected, $\Delta\alpha_i$ can be approximated as follows:

$$\Delta\alpha_i = \xi_i^{(1)}(\boldsymbol{q})\Delta p_{\mathrm{w}}^{(1)} + \xi_i^{(2)}(\boldsymbol{q})\Delta p_{\mathrm{w}}^{(2)} + \cdots + \xi_i^{(\mathrm{nw})}(\boldsymbol{q})\Delta p_{\mathrm{w}}^{(\mathrm{nw})} \tag{23}$$

where the parameterized coefficients $\xi_i^{(j)}$ (j=1, 2, …, $\mathrm{n_w}$) denote the sensitivities of α_i with respect to WPG at the nominal operating point. Thus, according to (21) and the eigenvalue sensitivity calculation method shown in [17], $\xi_i^{(j)}$ can be computed as follows:

$$\xi_k^{(j)} = \frac{\partial\alpha_k}{\partial p_{\mathrm{w}}^{(j)}} = \mathrm{Re}\left\{\boldsymbol{V}_{\mathrm{cp}}\begin{bmatrix} \dfrac{\partial\boldsymbol{A}_{\mathrm{o}}}{\partial p_{\mathrm{w}}^{(j)}} + \dfrac{\partial\boldsymbol{B}_{\mathrm{o}}}{\partial p_{\mathrm{w}}^{(j)}}\boldsymbol{D}_{\mathrm{c}}\boldsymbol{D}_{\mathrm{t}}\boldsymbol{C}_{\mathrm{o}} + \boldsymbol{B}_{\mathrm{o}}\boldsymbol{D}_{\mathrm{c}}\boldsymbol{D}_{\mathrm{t}}\dfrac{\partial\boldsymbol{C}_{\mathrm{o}}}{\partial p_{\mathrm{w}}^{(j)}} & \dfrac{\partial\boldsymbol{B}_{\mathrm{o}}}{\partial p_{\mathrm{w}}^{(j)}}\boldsymbol{D}_{\mathrm{c}}\boldsymbol{C}_{\mathrm{t}} & \dfrac{\partial\boldsymbol{B}_{\mathrm{o}}}{\partial p_{\mathrm{w}}^{(j)}}\boldsymbol{C}_{\mathrm{c}} \\ \boldsymbol{B}_{\mathrm{t}}\dfrac{\partial\boldsymbol{C}_{\mathrm{o}}}{\partial p_{\mathrm{w}}^{(j)}} & \boldsymbol{0} & \boldsymbol{0} \\ \boldsymbol{B}_{\mathrm{c}}\boldsymbol{D}_{\mathrm{t}}\dfrac{\partial\boldsymbol{C}_{\mathrm{o}}}{\partial p_{\mathrm{w}}^{(j)}} & \boldsymbol{0} & \boldsymbol{0} \end{bmatrix}\boldsymbol{U}_{\mathrm{cp}}\right\} \tag{24}$$

where $\boldsymbol{U}_{\mathrm{cp}}$ and $\boldsymbol{V}_{\mathrm{cp}}$ are the right and left eigenvectors of $\boldsymbol{A}_{\mathrm{cp}}$, respectively, and Re{·} denotes the operator for deriving the real part of the complex value inside the braces. Here, $\boldsymbol{A}_{\mathrm{o}}$, $\boldsymbol{B}_{\mathrm{o}}$, $\boldsymbol{C}_{\mathrm{o}}$, and their derivatives are evaluated as the open-loop power system operates at the nominal operating point ($\boldsymbol{p}_{\mathrm{w}}$=$\bar{\boldsymbol{p}}_{\mathrm{w}}$) so that they can be calculated beforehand, irrespective of the damping controllers, and remain constant during the optimization of the controllers' parameters. Specifically, the open source software — power system analysis toolbox (PSAT) incorporates a built-in function which can analytically derive $\boldsymbol{A}$, $\boldsymbol{B}$, and $\boldsymbol{C}$ at a given operating point [18]. Thus, based on this function, the derivatives of $\boldsymbol{A}_{\mathrm{o}}$, $\boldsymbol{B}_{\mathrm{o}}$ and $\boldsymbol{C}_{\mathrm{o}}$ in (24) are numerically computed by perturbing $\boldsymbol{p}_{\mathrm{w}}$ around $\bar{\boldsymbol{p}}_{\mathrm{w}}$. In other words, $\xi_i^{(j)}$ is exclusively and analytically calculable from the damping controllers' tunable parameters according to (24).

Following the properties of probabilistic calculation shown in the Appendix A, the pdf of α_i can be readily deduced based on (11), (12), and (23), as follows:

$$f^{(i)}(\alpha_i) = \sum_{t1=1}^{3}\sum_{t2=1}^{3}\cdots\sum_{tnw=1}^{3} c_{\mathrm{s}}\, g\left(\mu_{\mathrm{s}}, \sigma_{\mathrm{s}}, \alpha_i\right) \tag{25}$$

where c_{s}, μ_{s}, and σ_{s} are the symbolic replacements of the following expressions:

$$c_{\mathrm{s}} = c_{t1}^{(1)} c_{t2}^{(2)} \cdots c_{tnw}^{(\mathrm{nw})} \tag{26}$$

$$\mu_{\mathrm{s}} = \alpha_{i0} + \xi_i^{(1)}\mu_{t1}^{(1)} + \xi_i^{(2)}\mu_{t2}^{(2)} + \cdots \xi_i^{(\mathrm{nw})}\mu_{tnw}^{(\mathrm{nw})} \tag{27}$$

$$\sigma_{\mathrm{s}} = \sqrt{\left(\xi_i^{(1)}\sigma_{t1}^{(1)}\right)^2 + \left(\xi_i^{(2)}\sigma_{t2}^{(2)}\right)^2 + \cdots + \left(\xi_i^{(\mathrm{nw})}\sigma_{tnw}^{(\mathrm{nw})}\right)^2} \tag{28}$$

Here, the variables '*t1*', '*t2*', …, '*tnw*' are used for indexing, as was the case for '*t*' in (11). Then, the corresponding cdf of α_i is computed as follows:

$$\begin{aligned} F_1^{(i)}(\alpha_i) &= \int_{-\infty}^{\alpha_i} f^{(i)}(x)dx \\ &= \sum_{t1=1}^{3}\sum_{t2=1}^{3}\cdots\sum_{tnw=1}^{3} c_{\mathrm{s}}\int_{-\infty}^{\frac{\alpha_i-\mu_{\mathrm{s}}}{\sigma_{\mathrm{s}}}} g\left(0,1,x\right)dx \\ &= \sum_{t1=1}^{3}\sum_{t2=1}^{3}\cdots\sum_{tnw=1}^{3} c_{\mathrm{s}} G\left(\frac{\alpha_i-\mu_{\mathrm{s}}}{\sigma_{\mathrm{s}}}\right) \end{aligned} \tag{29}$$

where $G(\cdot)$ is the cdf of the standard Gaussian function. Based on equations (12) and (24)-(29), the cdf of α_i can be analytically and quickly evaluated given the damping controllers' parameters ($\boldsymbol{q}$); the time-consuming sampling method (e.g., LHS) is no longer necessary for this probabilistic computation. Moreover, it can be easily inferred that the derivatives of the damping's cdf with respect to $\boldsymbol{q}$ are analytically calculable. These merits will significantly benefit the process to solve the parameter optimization problem, which is constructed based on the cdf of α_i. Particularly, it should be kept in mind that the analytic calculations deduced above are applicable just in the case of mutually independent wind power sources. The convolution operation to deriving (25) is no longer feasible in the more general situations with correlated wind power. However, improving the proposed method to consider non-zero correlations among wind power sources is a nontrivial work which deserves further considerable research efforts.

B. Squared Relative Frequency Deviation of Critical Inter-Area Mode and its Probability Distribution

Another type of random variable considered in this paper relates to the frequency deviation of the critical inter-area mode due to the introduction of damping controllers. The squared

relative frequency deviation of the *i*th critical inter-area mode is defined as follows:

$$D_i = \left(\frac{\omega_i - \omega_{i\text{op}}}{\omega_{i\text{op}}} \right)^2 \tag{30}$$

where ω_i is the imaginary part of the *i*th critical inter-area mode and $\omega_{i\text{op}}$ represents ω_i when no damping controller is installed (open-loop). Analogous to α_i, the relationship between D_i and $\boldsymbol{p}_\text{w}$ can be linearly approximated in the following manner:

$$D_i = D_{i0} + \rho_i^{(1)} \Delta p_\text{w}^{(1)} + \rho_i^{(2)} \Delta p_\text{w}^{(2)} + \cdots + \rho_i^{(\text{nw})} \Delta p_\text{w}^{(\text{nw})} \tag{31}$$

where D_{i0} denotes the evaluation of D_i as $\boldsymbol{p}_\text{w}=\bar{\boldsymbol{p}}_\text{w}$, and $\rho_i^{(j)}$ (j=1, 2, …, n_w) is the derivative of D_i with respect to $p_\text{w}^{(j)}$. Here, ω_i ($\omega_{i\text{op}}$) and α_i can actually share almost the same computing process as they are equipotent in the eigenvalue calculation. Moreover, (30) is obviously an explicit and differentiable function with respect to ω_i and $\omega_{i\text{op}}$. Thus, by referring to the calculations concerning α_i in the previous subsection, it can be readily understood that D_{i0} and $\rho_i^{(j)}$ are exclusively determined by the damping controllers' parameters; indeed, they are the analytically differentiable functions of $\boldsymbol{q}$, but are not shown in this paper due to space limitations.

Based on (31), the cdf of the random variable D_i is derived as follows:

$$F_2^{(i)}(D_i) = \sum_{t1=1}^{3} \sum_{t2=1}^{3} \cdots \sum_{tnw=1}^{3} c_\text{ss} G\left(\frac{D_i - \mu_\text{ss}}{\sigma_\text{ss}} \right) \tag{32}$$

where c_ss, μ_ss, and σ_ss denote the following expressions:

$$c_\text{ss} = c_{t1}^{(1)} c_{t2}^{(2)} \cdots c_{tnw}^{(\text{nw})} \tag{33}$$

$$\mu_\text{ss} = D_{i0} + \rho_i^{(1)} \mu_{t1}^{(1)} + \rho_i^{(2)} \mu_{t2}^{(2)} + \cdots \rho_i^{(\text{nw})} \mu_{tnw}^{(\text{nw})} \tag{34}$$

$$\sigma_\text{ss} = \sqrt{\left(\rho_i^{(1)} \sigma_{t1}^{(1)}\right)^2 + \left(\rho_i^{(2)} \sigma_{t2}^{(2)}\right)^2 + \cdots + \left(\rho_i^{(\text{nw})} \sigma_{tnw}^{(\text{nw})}\right)^2} \tag{35}$$

Specifically, the two merits with respect to computing efficiency associated with the damping's cdf are also preserved by the cdf of D_i. Furthermore, the cdfs of α_i and D_i also make quite obvious sense in the damping control of the inter-area modes. Therefore, the subsequent section will focus on these two types of random variables to construct the optimization problem for tuning the damping controller parameters.

IV. Tuning of Damping Controller Parameters Based on Stochastic Optimization

As mentioned previously, if an inter-area mode is placed in the complex plane, its position will be stochastic due to the introduction of WPG in the power system, which randomly alters the steady-state operating point. Hence, in this section, the parameters ($\boldsymbol{q}$) of the damping controllers (wide-area PSSs) are simply tuned to optimize the 'stochastic position' of the critical inter-area modes. First, it should be clear that the cdf of α_i represents the cumulative probability of the damping of the *i*th critical inter-area mode being smaller than α_i; D_i measures the extent of the *i*th critical inter-area mode's frequency deviation caused by the damping controllers and thus its cdf stands for the cumulative probability of the deviation extent less than D_i.

According to the above interpretation of the cdfs of α_i and D_i, the optimal 'stochastic position' of the inter-area modes can be achieved by solving the following optimization problem:

$$\max_{\boldsymbol{q}} \sum_{i \in \Omega} [W_1^{(i)} F_1^{(i)}(\alpha_{spec}^{(i)}) + W_2^{(i)} F_2^{(i)}(D_{spec}^{(i)})] \tag{36}$$

$$\text{s.t.} \qquad \mathbf{q}_\text{min} \le \boldsymbol{q} \le \mathbf{q}_\text{max} \tag{37}$$

where $\alpha_{spec}^{(i)}$ is the specified constant indicating satisfactory damping of the *i*th inter-area mode and $D_{spec}^{(i)}$ is the preferred upper bound of the frequency deviation extent; $W_1^{(i)}$ and $W_2^{(i)}$ are the weights of $F_1^{(i)}(\cdot)$ and $F_2^{(i)}(\cdot)$, respectively; $\mathbf{q}_\text{min}$ and $\mathbf{q}_\text{max}$ are the lower and upper bounds of $\boldsymbol{q}$, respectively; and Ω is the set collecting the indexes of the critical inter-area modes. This formulated optimization is meaningful with respect to damping control design because it simultaneously enhances the probabilities of two types of favorable control effects (events): the tuned controllers can control a critical inter-area mode to obtain satisfactory damping; and the damping controllers' induced frequency deviation of a critical inter-area mode with respect to the open-loop state is less than the specified value (to avoid considerable impacts on the synchronous torque of generators related to the transient stability issue).

Section III addressed the analytic properties of $F_1^{(i)}(\cdot)$, $F_2^{(i)}(\cdot)$, and their derivatives with respect to $\boldsymbol{q}$. Therefore, gradient descent-based algorithms can be used to solve the optimization (36)-(37). Specifically, a typical such algorithm is sequential quadratic programming (SQP), which is a mature and efficient method to solve constrained nonlinear programming problems. It is employed in this paper to search the optimal parameters of the damping controllers.

V. Simulations and Analysis

To verify the performance of the proposed method for designing probabilistically robust damping controllers, simulations are conducted with a modified IEEE 10-machine 39-bus system. In particular, to make the verification logical and comprehensive, simulation results as well as proper comparisons are presented in detail in terms of four aspects. First, the computational efficiency of the proposed method is simulated and its overwhelming advantage over the sampling based method is demonstrated (Subsection V-B). Then, as the necessary condition to ensure the desired design results, the accuracy of the proposed probabilistic eigenvalue calculation is validated (Subsection V-C). Furthermore, control effects comparisons are conducted with the WPSSs designed by the proposed method, the probabilistically robust method in [7], and the traditional H_∞ index-based design method, respectively (Subsection V-D). Finally, the impacts of variable communication time delays on performance of WPSSs designed by proposed method are analyzed (Subsection V-E).

A. Test System

The test system shown in Fig. 3 is derived by modifying the standard IEEE 10-machine 39-bus system. Specifically, three identical wind farms (WFs) are connected to Bus-14, -16, and -17, respectively, through short transmission lines. The pdfs of these three WFs are based on the real wind power data from the

SaskPower Corporation, located in Saskatchewan, Canada [19]. Moreover, three active power loads are also connected to Bus-14, -16, and -17, respectively, and each consumes the expected power output (about 330 MW) of the nearby WF. Other system components (e.g., synchronous generators, exciters, transmission lines, loads, etc.) use models and parameters from [20].

When the total WPG in the steady state deviates from expectations (i.e., 3×330=990 MW), the deviation is supposed to be compensated for in a proportional manner by the synchronous generators G1 (25%), G6 (30%), and G7 (45%) so as to maintain balance between overall power generation and demand of the system. Furthermore, irrespective of the operating point changes owing to variations in WPG, eigen-analysis shows that four poorly damped inter-area oscillation modes consistently exist in this system. Table I lists these modes for the nominal operating point and the associated synchronous generators that have relatively large participation factors. Thus, four WPSSs with the structures shown in Fig. 2 are installed in G7, G5, G9, and G4, respectively, to enhance the damping of these inter-area modes. According to the residue analysis, wide-area measurements of active power in transmission lines #22-35, #19-16, #29-38 and #8-9 are selected as the feedback signals for the four respective WPSSs. In this simulated case, WPSS1, WPSS2 and WPSS4 employ the dedicated optical-fiber channels to transmit the remote signals. The expected time delays in these feedback control loops are hypothetically identical to be 100 ms [15]. Particularly, WPSS3 uses the nearby feedback signal so that no signal transmission latency is assumed. Furthermore, the design parameters $\alpha_{spec}^{(i)}$ are set to be -0.25, -0.25, -0.25, and -0.20 while $D_{spec}^{(i)}$ are selected to be 0.001, 0.001, 0.001, and 0.01. The weights $W_1^{(i)}$ and $W_2^{(i)}$ are then chosen to be 0.7, 0.7, 0.7, 0.7 and 0.3, 0.3, 0.3, 0.3 respectively. Finally, the $\mathbf{q}_{\min}$ and $\mathbf{q}_{\max}$ of gain (K) are set to be 0 and 10, and time constants T_1, T_2, T_3, T_4 are set to be 0, 0, 0, 0 and 1, 1, 1, 1 respectively.

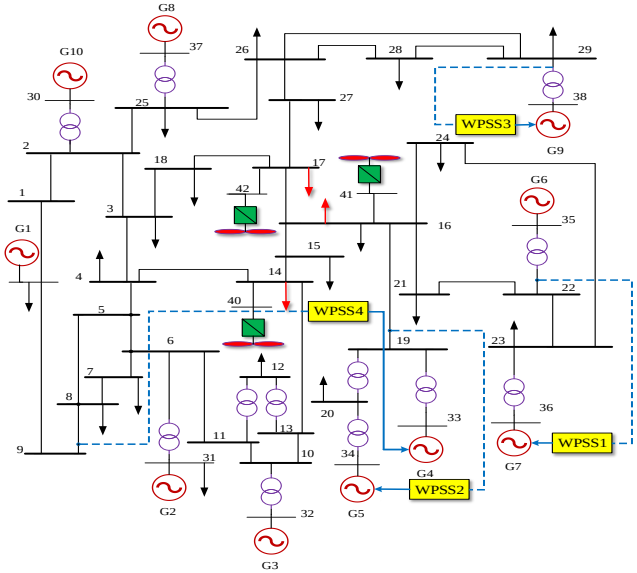

Fig. 3. Modified IEEE 10-machine 39-bus system

TABLE I
CRITICAL INTER-AREA MODES OF OPEN-LOOP SYSTEM

Mode No.	Eigenvalue	Damping Ratio	Generators
1	-0.1250±5.4967	0.0227	G2,G5,G6,G7
2	-0.1494±5.0561	0.0295	G2,G3,G5,G9
3	-0.1270±4.3579	0.0291	G4,G5,G8,G9
4	-0.0623±3.1703	0.0196	G1,G4,G5,G7

B. Computational Efficiency of Searching Optimal Parameters of WPSSs by Proposed Method

As described in Sections II and III, the cdfs of α_i and D_i as well as their derivatives with respect to the tunable parameters of the WPSSs can be evaluated directly, which makes solving the optimization problem (36)-(37) quite efficient using the gradient descent-based algorithm (i.e., SQP). To verify this, the optimization is run 10 times with 10 different initial solutions randomly generated within the range from $\mathbf{q}_{\min}$ and $\mathbf{q}_{\max}$. Specifically, Fig. 4 shows that, after around 10 iterations, all of the searching processes finally converge. Thus, although this convergence phenomenon cannot yet be theoretically guaranteed for other initial solutions, the searching runs provide solid evidence that solving the optimization by SQP provides quite excellent convergence. Moreover, Table II indicates the total time required by each run to converge as well as the average time cost per iteration in each run. These times are fairly consistent and short, which confirms the efficiency of deriving the optimal parameters of the WPSSs by the proposed method.

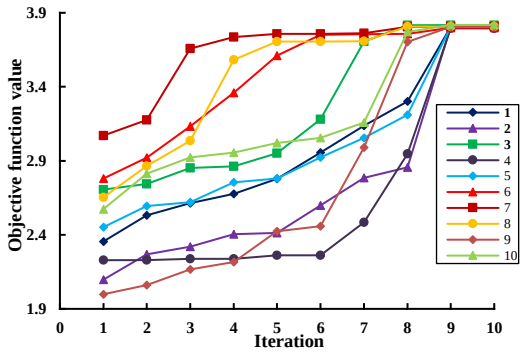

Fig. 4. Searching processes from 10 different initial solutions by SQP

TABLE II
COMPUTATION TIMES OF 10 DIFFERENT INITIAL SOLUTIONS USING THE PROPOSED METHOD

Initial Solution	Iteration Time (s)	Total Time (s)
1	0.4351	4.3510
2	0.4623	4.1607
3	0.4416	3.9749
4	0.4854	5.2867
5	0.4423	4.4227
6	0.3679	3.6788
7	0.4712	4.7128
8	0.4687	5.6244
9	0.5069	5.5759
10	0.5298	5.8157
Mean Value	0.4611	4.7604

For comparison, a relatively efficient sampling technique, LHS [21], is employed to evaluate the cdfs of α_i and D_i and their derivatives. The number of samplings in this use of LHS is 800. Moreover, because no analytical expression of the cdfs can be

obtained by LHS, the derivatives are computed based on the method of parameter perturbation. Then, the optimization problem (36)-(37) is also solved by SQP with the LHS-based cdfs (derivatives). Here, this solving process is only executed one time. Although the searching converges after 11 iterations, the total computational time is 290.6750 s with each iteration taking an average of 26.4250 s. Comparing these data with those associated with the proposed method clearly shows the overwhelming advantage of the latter in terms of computational efficiency. In other words, the proposed direct calculation of the cdfs in this paper is obviously effective and is also a unique contribution in terms of favorable computational efficiency.

C. Accuracies of the CDFs Derived by the Proposed Calculations

In this paper, the cdfs of α_i and D_i can be directly derived by the proposed explicit expressions (29) and (32). Because the cdfs are used to form the objective function that quantitatively measures control effects of the WPSSs, the accuracy of the cdfs derived from (29) and (32) has a very important influence on the quality of tuning of the WPSSs based on the objective function. Therefore, in this subsection the proposed calculations are compared with benchmarks obtained by Monte Carlo simulations (MCS; simple random sampling). The number of samplings used here is 10000.

TABLE III
OPTIMAL PARAMETERS OF WPSSS BY THE PROPOSED METHOD

WPSS	*K*	T_1	T_2	T_3	T_4
G7	1.9748	0.0821	0.8499	0.1187	0.8159
G5	0.9189	0.2865	0.7519	0.3597	0.8796
G9	0.2668	0.1081	0.8628	0.2246	0.9301
G4	1.8988	0.0667	0.6287	0.1064	0.6094

TABLE IV
$F_1^{(i)}(\alpha_{spec}^{(i)})$ OF FOUR INTER-AREA MODES OBTAINED BY MCS AND THE PROPOSED METHOD

Mode No.	MCS	Proposed Method	Relative Error	RMS Error
1	0.9561	0.9621	0.63%	0.0118
2	0.9959	1.0000	0.41%	0.0130
3	1.0000	1.0000	0	0.0106
4	0.8537	0.8579	0.49%	0.0091

TABLE V
$F_2^{(i)}(D_{spec}^{(i)})$ OF FOUR INTER-AREA MODES OBTAINED BY MCS AND THE PROPOSED METHOD

Mode No.	MCS	Proposed Method	Relative Error	RMS Error
1	0.9757	0.9813	0.57%	0.0119
2	0.9902	0.9943	0.41%	0.0114
3	0.9816	0.9904	0.90%	0.0097
4	0.9541	0.9632	0.95%	0.0095

The cdfs of α_i and D_i are computed when the installed WPSSs have the optimal parameters (Table III), which are found in the previous subsection. Then, the approximated cdfs obtained by the proposed calculations and their benchmarks are compared in Figs. 5 and 6. Both α_i and D_i clearly have approximated cdfs that are very close to the real cdfs. Specifically, depending on the selection of design parameters $\alpha_{spec}^{(i)}$ and

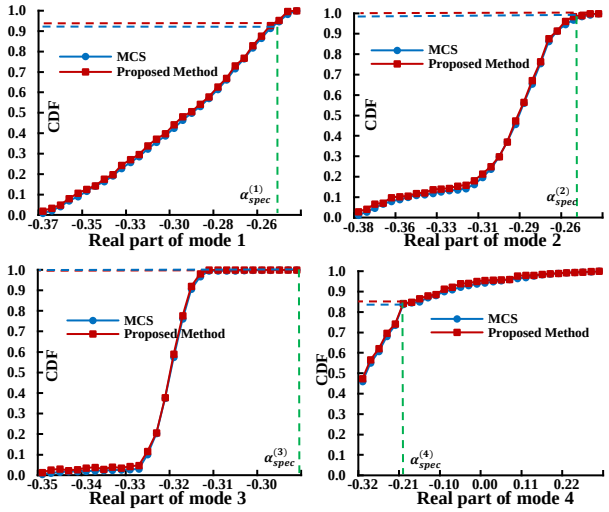

Fig. 5. The α_i cdfs of four inter-area modes obtained by MCS and the proposed method

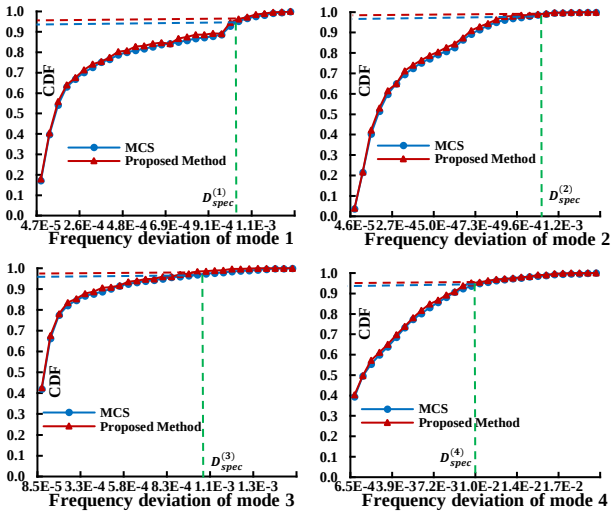

Fig. 6. The D_i cdfs of all four inter-area modes obtained by MCS and the proposed method

$D_{spec}^{(i)}$ in Subsection V-A, the corresponding cumulative probability values are derived (mapped) based on the cdfs of α_i and D_i. Tables IV and V show these values calculated from the approximated and the real cdfs, respectively, as well as the relative error between them and the root mean square (RMS) error over the whole region of the cdf curve. For all four inter-area modes, this method has fairly favorable accuracies when computing the cumulative probabilities of $\alpha_i<\alpha_{spec}^{(i)}$ and $D_i<D_{spec}^{(i)}$ using expressions (29) and (32). Therefore, the objective function can be accurately evaluated and so minimizing it to tune the WPSSs clearly makes sense.

D. Control Results of WPSSs Tuned by the Proposed Method

Control results for WPSSs with the optimal parameters were presented in the previous subsection (i.e., the cdfs of α_i and D_i). However, to comparatively highlight the effectiveness of the proposed method for dealing with uncertain wind power, two competitive methods are also used in this subsection to tune the WPSSs. One is the recently proposed differential evolution based probabilistically-robust (DEPR) method [7], which evaluates the cdfs of α_i and D_i using LHS and solves the opti-

mization (36)-(37) using a customized differential evolution algorithm. The second is another H_∞ index-based method that, besides meeting the same damping and frequency drift requirements, tunes the WPSSs to simultaneously maximize the closed-loop system's robustness against model uncertainties in the nominal operating condition [22].

The indexes $F_1^{(i)}(\alpha_{spec}^{(i)})$ and $F_2^{(i)}(D_{spec}^{(i)})$ are evaluated for the four inter-area modes of the closed-loop system when the two competitive methods are respectively used for tuning the WPSSs (Tables VI and VII). Moreover, these indexes were also evaluated in the previous subsection with the proposed method (Tables IV and V). The comparison shows that the WPSSs tuned by the proposed method can have nearly the same large probability as determined by the DEPR method in [7] to meet the required damping control effects as the system operating condition randomly varies due to wind power integration. In addition, Fig. 7 compares the pdfs of α_i obtained using the three respective tuning methods. All four inter-area modes obviously have comparatively large probability densities toward the leftmost direction of the x-axis (i.e., the heavily damped region) when the WPSSs tuned by the proposed method are used. In contrast, the WPSSs derived using the H_∞ index-based method result in the worst probability density distributions of the inter-area mode because the H_∞ (robustness) index created is only based on the local information around the nominal operating point and cannot consider large-scale uncertainties as well as their probability distributions. Furthermore, the proposed method provides tuned WPSSs with almost the same excellent robustness as those derived by the probabilistically robust method in [7]. However, the computational efficiency of the proposed method is much better than the DEPR method, as validated in subsection V-B. Therefore, the above comparisons support the conclusion that the proposed method can efficiently and accurately take into account the randomness of WPG in damping control design and tune the WPSSs to achieve very satisfactory robustness in terms of the desired probability distributions of concerned variables, e.g., the damping of inter-area modes.

TABLE VI
$F_1^{(i)}(\alpha_{spec}^{(i)})$ AND $F_2^{(i)}(D_{spec}^{(i)})$ OF FOUR INTER-AREA MODES BY THE DEPR METHOD

Mode No.	$F_1^{(i)}(\alpha_{spec}^{(i)})$	$F_2^{(i)}(D_{spec}^{(i)})$
1	0.9853 (-0.25)	0.9778 (0.001)
2	0.9998 (-0.25)	0.9985 (0.001)
3	1.0000 (-0.25)	0.9901 (0.001)
4	0.8736 (-0.20)	0.9703 (0.01)

TABLE VII
$F_1^{(i)}(\alpha_{spec}^{(i)})$ AND $F_2^{(i)}(D_{spec}^{(i)})$ OF FOUR INTER-AREA MODES BY THE H_∞ INDEX-BASED METHOD

Mode No.	$F_1^{(i)}(\alpha_{spec}^{(i)})$	$F_2^{(i)}(D_{spec}^{(i)})$
1	0.7861 (-0.25)	0.7850 (0.001)
2	0.7972 (-0.25)	0.8219 (0.001)
3	0.8825 (-0.25)	0.8031 (0.001)
4	0.6962 (-0.20)	0.7726 (0.01)

The nonlinear time domain simulations are conducted to further confirm the above analysis results. First, at a selected operating point, an instantaneous three-phase short circuit fault occurs at Bus 3 at 1.0 s and is self-cleared 150 ms later [23]. The relative power angles of G2 vs. G1 and G9 vs. G2 are selected to compare the control effects of WPSSs which are tuned by different methods. Figs. 8 and 9 show that the WPSSs tuned by the H_∞ index-based method just provide the least damping to the power angle oscillations among the three design methods; the proposed design method and the DEPR method, both have produced the WPSSs which quite analogously perform to rapidly damp the oscillations (i.e., the power angle oscillations can remarkably decay within 10 s). Therefore, the overwhelming advantage in the computational efficiency compared with the DEPR method makes the proposed method more attractive and competitive in the practical application.

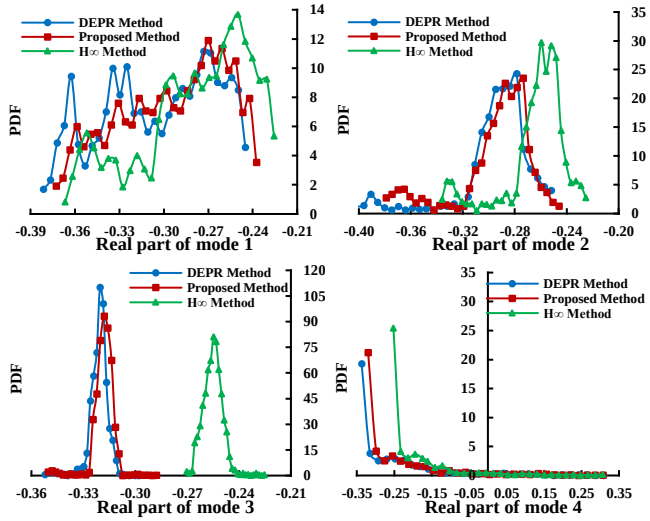

Fig. 7. The α_i pdfs of all four inter-area modes determined using three different tuning methods

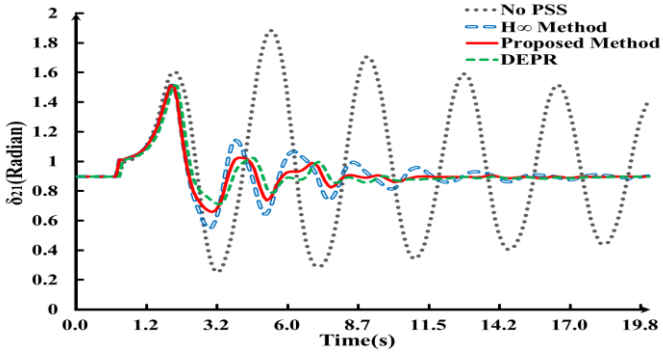

Fig. 8. Time domain response of δ_{21} with the three-phase short circuit fault

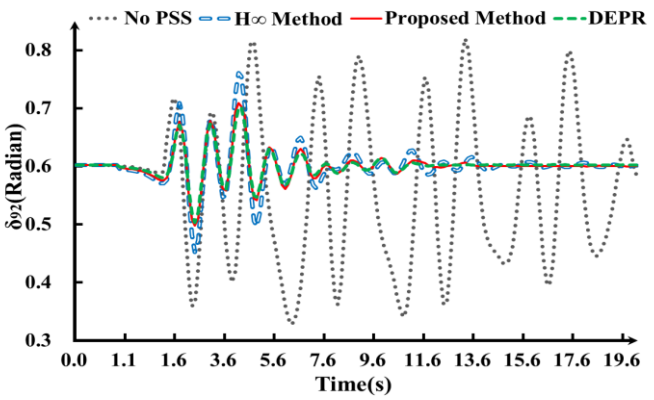

Fig. 9. Time domain response of δ_{92} with the three-phase short circuit fault

Besides the short-circuit fault, wind speed variations are also employed as disturbances to initiate the time domain simulation. For simplicity, only the wind speed of wind farm connected to Bus 40 is assumed to be variable while the other wind farms' wind speeds are fixed during the simulation. Moreover, Fig. 10 shows that the wind speed is supposed to change (jump) every ten seconds (here, it should be noted that at the start time point, the wind speed just finishes a jump from 10 to 12 m/s). The time interval of ten seconds means that the wind speed dynamics are essentially too slow to directly couple with the electromechanical dynamics of the system. Actually, they indirectly alter the system's small signal stability by changing the operating point, which however has been explicitly considered by the proposed control design. Figs. 11 and 12 clearly show that each wind speed jump corresponds to an operating point shift and the WPSSs can consistently work well to suppress the inter-area oscillations at all these operating points.

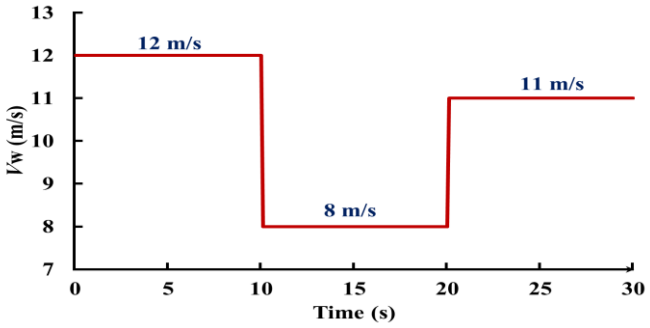

Fig. 10. The variable wind speed

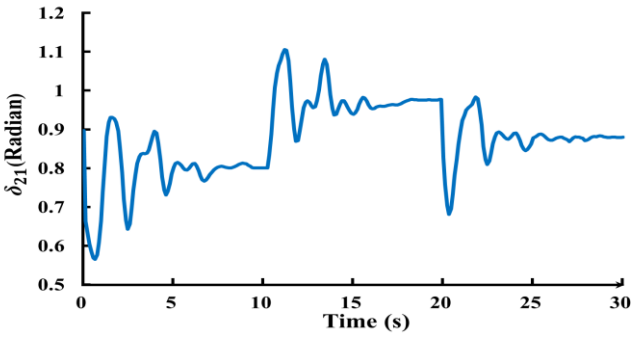

Fig. 11. Time domain response of δ_{21} with the variable wind speed

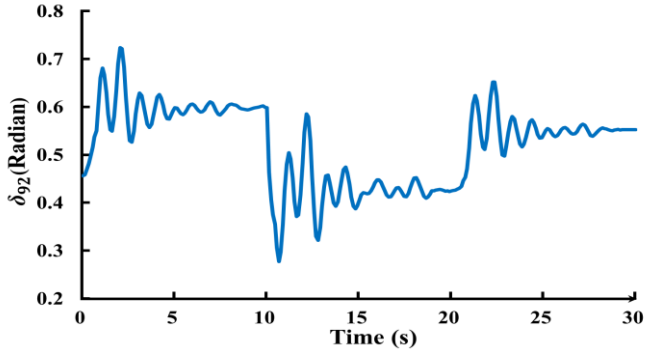

Fig. 12. Time domain response of δ_{92} with the variable wind speed

E. Impacts of Variable Communication Time Delays on Performance of WPSSs Designed by Proposed Method

TABLE VIII
$F_1^{(1)}(\alpha_{spec}^{(1)})$ AND $F_2^{(1)}(D_{spec}^{(1)})$ UNDER VARIABLE TIME DELAYS

Actual time delay	WPSSs (no time delay)		WPSSs (expected time delay)	
	$F_1^{(1)}(\alpha_{spec}^{(1)})$	$F_2^{(1)}(D_{spec}^{(1)})$	$F_1^{(1)}(\alpha_{spec}^{(1)})$	$F_2^{(1)}(D_{spec}^{(1)})$
0ms	0.9470	0.9631	0.9033	0.9206
50ms	0.9207	0.9244	0.9362	0.9347
100ms	0.8998	0.9036	0.9561	0.9757
150ms	0.8713	0.8834	0.9287	0.9380

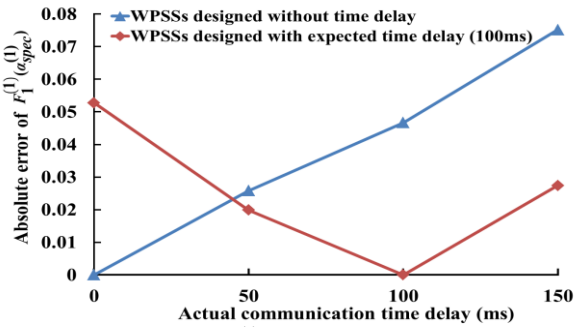

Fig. 13. The absolute error of $F_1^{(1)}(\alpha_{spec}^{(1)})$

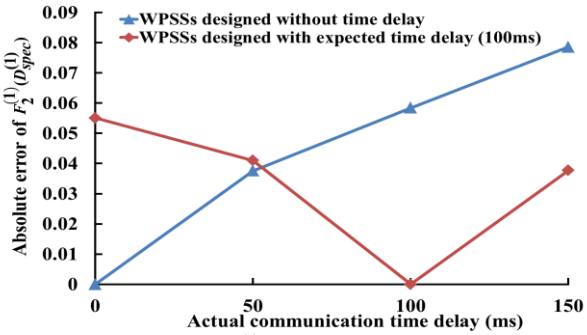

Fig. 14. The absolute error of $F_2^{(1)}(D_{spec}^{(1)})$

This subsection investigates the influences of variable time delays on the performance of WPSSs designed by the proposed method. It is known that the expected time delay of 100 ms has been used for the WPSSs design. Thus, the actual time delays of 0, 50, 100 and 150 ms are respectively simulated for the feedback control loops. For example, if the actual time delay is 50 ms, the signal channels of WPSS1, WPSS2 and WPSS4 have the same actual time delays being 50 ms. Here, the maximum of

150 ms is selected with the consideration of having employed the dedicated optical fiber communication system [15]. Table VIII takes the indexes $F_1^{(1)}(\alpha_{spec}^{(1)})$ and $F_2^{(1)}(D_{spec}^{(1)})$ as examples to show their values under the simulated actual time delays. Moreover, Figs. 13 and 14 illustrate the absolute errors between the indexes computed using the actual time delays and the ones which are derived with the expected time delay of 100 ms. Apparently, the errors should be zero as the actual time delay is 100 ms and they increase as the actual time delay deviates from 100 ms.

Comparatively, the WPSSs are also designed by the proposed method but without considering any time delay. The above two indexes as well as their absolute errors (with respect to the values computed without time delay) are correspondently computed and shown in Table VIII, Figs. 13 and 14. It is seen that in the worst case of time delay mismatch (actual: 150 ms and designed: 0 ms), the indexes' errors even rise to around 0.078 by the WPSSs derived without considering time delay. In contrast, the maximum error is less than 0.056 when the WPSSs are designed to take into account the expected time delay. Therefore, all these simulations have addressed that in the fine communication environments, modeling the expected time delay is an effective way to lower the adverse impacts of time delay's variability on the damping control effects.

VI. Conclusion

This paper employs a simple and effective Gaussian mixtures method (i.e., a linear combination of three Gaussian functions) to approximate the pdf of WPG. Based on the approximations, the novelties of the research works conducted in this paper are concluded, as follows:

1) The cdfs of two types of random variables (damping and squared relative frequency change ratio) associated with the concerned inter-area modes are analytically deduced, together with the analytical derivatives of the cdfs with respect to the tunable parameters of the WPSSs;

2) An optimization problem which uses these cdfs to compose the objective function is constructed to optimize the parameters of the WPSSs. Apparently, the probabilities that the concerned inter-area modes have satisfactory damping and that the related frequency changes due to WPSSs are less than the specified values can be simultaneously increased by the optimized WPSSs;

3) Since the objective function comprised of the cdfs is analytically differentiable with respect to the WPSSs' parameters, the proposed optimization can be quite efficiently solved by the mathematical programming approaches (e.g. the SQP method).

Consequently, the design efficiency of the proposed method and the expected performance of the optimized WPSSs are successfully verified in a modified IEEE 10-machine 39-bus system.

Appendix

A. General Properties of the Probabilistic Calculation

Assume that x_1 and x_2 are two independent random variables and their pdfs are defined as $f^{(x_1)}(\cdot)$ and $f^{(x_2)}(\cdot)$, respectively. An additional random variable x_3 is the linear function of x_1 and x_2 and its pdf is $f^{(x_3)}(\cdot)$. Therefore, three general properties of probability calculation are introduced as follows [11]:

1) If the equation $x_3=ax_1$ is satisfied where a is constant, then $f^{(x_3)}(x_3)=f^{(x_1)}(x_3/a)/a$.

2) If the linear equation $x_3=x_1+x_2$ is satisfied, then $f^{(x_3)}(x_3)=f^{(x_1)}(x_3)\otimes f^{(x_2)}(x_3)$ is workable, where $\otimes$ represents the convolution operator.

3) If x_1 and x_2 both fit the Gaussian distribution and $x_3=x_1+x_2$ is also satisfied, then $f^{(x_3)}(\cdot)$ is still the Gaussian distribution function with its expectation equal to the sum of expectations of x_1 and x_2, and its variance equivalent to the sum of the variances of x_1 and x_2.

B. Simplified Model of DFIG based Wind Turbine

Due to the primary concern of electromechanical dynamics, a simplified model of DFIG based wind turbine is applied in this paper [24]: i. dynamics of stator and dc-link capacitor are neglected; ii. rotor side converter (RSC) and grid side converter (GSC) are ideal, no power loss and instantaneous response to control reference order; iii. GSC is ideally controlled to make no reactive power exchange with grid during the transients; iv. a lumped-mass turbine and generator shaft is used. Thus, the simplified model can be mathematically described, as follows:

$$\frac{1}{\omega_b}\frac{de_d}{dt}=-\frac{1}{T_0}[e_d-(X-X')i_{qs}]+s\omega_s e_q-\omega_s\frac{L_m}{L_r+L_m}v_{qr} \quad (38)$$

$$\frac{1}{\omega_b}\frac{de_q}{dt}=-\frac{1}{T_0}[e_q+(X-X')i_{ds}]-s\omega_s e_d+\omega_s\frac{L_m}{L_r+L_m}v_{dr} \quad (39)$$

$$\frac{d\omega_r}{dt}=\frac{1}{2H}[\frac{p_w}{\omega_r}-\frac{e_d i_{ds}+e_q i_{qs}}{\omega_s}] \quad (40)$$

$$p_w=p_{w\_ori}\times C_p(\omega_r) \quad (41)$$

$$v_{ds}=X'i_{qs}+e_d \quad (42)$$

$$v_{qs}=-X'i_{ds}+e_q \quad (43)$$

$$i_{dr}=\frac{1}{\omega_s L_m}e_q+\frac{L_m}{L_r+L_m}i_{ds} \quad (44)$$

$$i_{qr}=\frac{-1}{\omega_s L_m}e_d+\frac{L_m}{L_r+L_m}i_{qs} \quad (45)$$

where e is the internally generated voltage; v_s is the stator voltage; v_r is the rotor voltage; i_s is the stator current; i_r is the rotor current; the symbols 'd' and 'q' in the subscripts of these variables mean the relevant variables are the d-axis and q-axis components, respectively; ω_b, ω_r and ω_s are the system speed base, the rotor speed and the synchronous speed, respectively; V_w is the wind speed; $p_{w\_ori}(V_w)$ is the wind power coming toward the wind turbine; p_w is the converted mechanical power on the shaft according to the conversion coefficient $C_p(\omega_r)$; H is the shaft inertia constant; T_0 denotes the transient open-circuit time constant; L_m and L_r are the magnetizing inductance and rotor leakage inductance, respectively.

The stator voltage oriented decoupling strategy is employed by the RSC controllers which are actually two typical proportional-integral (PI) regulators. One regulates v_{dr} to realize zero

reactive power output of the stator, and another controls v_{qr} to enable the active power output of DFIG following the maximum wind power order (which is offered by the maximum power point tracking (MPPT) algorithm).

REFERENCES

[1] Bo Yuan, Ming Zhou, and Gengyin Li, "Stochastic small-signal stability of power systems with wind power generation," *IEEE Trans. Power Syst.*, vol. 30, no. 4, pp. 1680-1689, Jul. 2015.

[2] Mohamed Edrah, Kwok L. Lo, and Olimpo Anaya-Lara, "Impacts of high penetration of DFIG wind turbines on rotor angle stability of power systems," *IEEE Trans. Sustain. Energy*, vol. 6, no. 3, pp. 759-766, Jul. 2015.

[3] D. Gautam, V. Vittal, and T. Harbour, "Impact of increased penetration of DFIG-based wind turbine generators on transient and small signal stability of power systems," *IEEE Trans. Power Syst.*, vol. 24, no. 3, pp. 1426-1434, Aug. 2009.

[4] T. Surinkaew and I. Ngamroo, "Coordinated robust control of DFIG wind turbine and PSS for stabilization of power oscillations considering system uncertainties," *IEEE Trans. Sustain. Energy*, vol. 5, no. 3, pp. 823-833, Jul. 2014.

[5] R. Preece and J. V. Milanovic, "Tuning of a damping controller for multiterminal VSC-HVDC grids using the probabilistic collocation method," *IEEE Trans. Power Del.*, vol. 29, no. 1, pp. 318-326, Feb. 2014.

[6] C. A. Juarez, J. L. Rueda, I. Erlich, and D. G. Colome, "Probabilistic approach-based wide-area damping controller for small-signal stability enhancement of wind-thermal power systems," in *IEEE Power and Energy Society General Meeting*, Detroit, USA, 2011, pp. 1-4.

[7] D. P. Ke and C. Y. Chung, "Design of probabilistically-robust wide-area power system stabilizers to suppress inter-area oscillations of wind integrated power systems," *IEEE Trans. Power Syst.*, vol. 31, no. 6, pp. 4297-4309, Nov. 2016.

[8] H. Huang and C. Y. Chung, "Coordinated damping control design for DFIG-based wind generation considering power output variation," *IEEE Trans. Power Syst.*, vol. 27, no. 4, pp. 1916-1925, Nov. 2012.

[9] S. Q. Bu, W. Du, and H. F. Wang, "Probabilistic analysis of small-signal stability of large-scale power systems as affected by penetration of wind generation," *IEEE Trans. Power Syst.*, vol. 27, no. 2, pp. 762-770, May 2012.

[10] Z. W. Wang, C. Shen, and F. Liu, "Probabilistic analysis of small signal stability for power systems with high penetration of wind generation," *IEEE Trans. Sustain. Energy*, vol. 7, no. 3, pp. 1182-1193, Jul. 2016.

[11] D. P. Ke, C. Y. Chung, and Y. Z. Sun, "A novel probabilistic optimal power flow model with uncertain wind power generation described by customized Gaussian mixture model," *IEEE Trans. Sustain. Energy*, vol. 7, no. 1, pp. 200-212, Jan. 2016.

[12] Z. W. Wang, C. Shen, and F. Liu, "Probabilistic analysis of small signal stability for power systems with high penetration of wind generation," *IEEE Trans. Sustain. Energy*, vol. 7, no. 3, pp. 1182-1193, Jul. 2016.

[13] S. Q. Bu, W. Du, and H. F. Wang, "Probabilistic analysis of small-signal rotor angle/voltage stability of large-scale AC/DC power systems as affected by grid-connected offshore wind generation," *IEEE Trans. Power Syst.*, vol. 28, no. 4, pp. 3712-3719, Nov. 2013.

[14] D. P. Ke and C. Y. Chung, "An inter-area mode oriented pole-shifting method with coordination of control efforts for robust tuning of power oscillation damping controllers," *IEEE Trans. Power Syst.*, vol. 27, no. 3, pp. 1422-1432, Aug. 2012.

[15] B. Naduvathuparambil, M. C. Valenti, and A. Feliachi, "Communication delays in wide area measurement systems," in *Proceedings of the Thirty-Fourth Southeastern Symposium on System Theory*, Huntsville, Alabama, 2002, pp. 371-375.

[16] S. Ghosh, K. A. Folly, and A. Patel, "Synchronized versus non-synchronized feedback for speed-based wide-area PSS: effect of time-delay," *IEEE Trans. Smart Grid*, early access.

[17] K. W. Wang, C. Y. Chung, and C. T. Tse, "Multimachine eigenvalue sensitivities of power system parameters," *IEEE Trans. Power Syst.*, vol. 15, no. 2, pp. 741-747, May 2000.

[18] Federico Milano. Power System Analysis Toolbox [DB/OL]. http://faraday1.ucd.ie/psat.html.

[19] SaskPower, Saskatoon, Saskatchewan, Canada [Online]. Available: http://www.saskpower.com/our-power-future/our-electricity/our-electrical-system/.

[20] Anantha Pai, *Energy Function Analysis for Power System Stability*, US: Springer, 1989.

[21] H. Yu, C. Y. Chung, K. P. Wong, and J. H. Zhang, "Probabilistic load flow evaluation with hybrid Latin Hypercube Sampling and Cholesky decomposition," *IEEE Trans. Power Syst.*, vol. 24, no. 2, pp. 661-667, May 2009.

[22] C. Y. Chung, C. T. Tse, and A. K. David, "Partial pole placement of H∞ based PSS design using numerator-denominator perturbation representation," *IEE Proceedings – Generation, Transmission and Distribution*, vol. 148, no. 5, pp. 413-419, Sep. 2001.

[23] C. Canizares, T. Fernandes, and E. Geraldi, "Benchmark modes for the analysis and control of small-signal oscillatory dynamics in power systems," *IEEE Trans. Power Syst.*, vol. 32, no. 1, pp. 715-722, Jan. 2017.

[24] O. Anaya-Lara, N. Jenkins, J. Ekanayake, P. Cartwright, and M. Hughes, *Wind Energy Generation—Modelling and Control*, Wiley, 2009.

Jingsen Zhou received the B.S degree in Electrical Engineering in 2012 from Wuhan University, Wuhan, China. Currently, he is pursuing the Ph.D. degree in the School of Electrical Engineering, Wuhan University. From 2016 to 2017, he is funded as a joint Ph.D. student in the Department of Electrical and Computer Engineering at the University of Saskatchewan, Saskatoon, SK, Canada. His research interests are in power system stability and control, wind power.

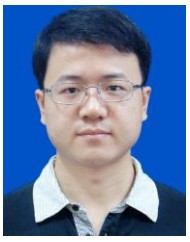

Deping Ke received the B.S degree in Electrical Engineering in 2005 from Huazhong University of Science and Technology, Wuhan, China, and the Ph.D. degree in Electrical Engineering from The Hong Kong Polytechnic University in 2012. Currently, he is an Associate Professor with the School of Electrical Engineering, Wuhan University, China. His research interests are in power system dynamics and control, and economic operation of power systems.

C. Y. Chung (M'01–SM'07–F'16) received the Ph.D. degree in electrical engineering from The Hong Kong Polytechnic University in 1999. He is currently a Professor and the SaskPower Chair in Power Systems Engineering in the Department of Electrical and Computer Engineering at the University of Saskatchewan, Saskatoon, SK, Canada. His research interests include power system stability/control, planning and operation, computational intelligence applications, power markets, and electric vehicle charging. Dr. Chung is an Editor of the IEEE TRANSACTIONS ON SUSTAINABLE ENERGY and the IEEE TRANSACTIONS ON POWER SYSTEMS. He is also an Editorial Board Member of IET GENERATION, TRANSMISSION & DISTRIBUTION. He is also a Member-at-Large (Smart Grid) of IEEE PES Governing Board and the IEEE PES Region 10 North Chapter Representative.

Yuanzhang Sun (M'99-SM'01) received the B.S. degree from Wuhan University of Hydro and Electrical Engineering, Wuhan, China, in 1982, the M.S. degree from the Electric Power Research Institute(EPRI), Beijing, China, in 1984, and the Ph.D. degree in electrical engineering from Tsinghua University, Beijing, in 1988. Currently, he is a Professor of the School of Electrical Engineering at Wuhan University, and a Chair Professor of the Department of Electrical Engineering and Vice Director of the State Key Lab of Power System Control and Simulation at Tsinghua University. His main research interests are in the areas of power system dynamics and control, wind power, voltage stability and control, and reliability.